Journal of Power Sources 202 (2012) 85–91

Contents lists available at SciVerse ScienceDirect

Journal of Power Sources

journal homepage: www.elsevier.com/locate/jpowsour

Self-ordered titania nanotubes and flat surfaces as a support for the deposition of nanostructured Au–Ni catalyst: Enhanced electrocatalytic oxidation of borohydride

L. Tamašauskaitė-Tamašiūnaitė [a,*], A. Balčiūnaitė [a,b], D. Šimkūnaitė [a], A. Selskis [a]

[a] State Research Institute, Center for Physical Sciences and Technology, Institute of Chemistry, A. Goštauto 9, LT-01108 Vilnius, Lithuania
[b] Faculty of Chemistry, Vilnius University, Naugarduko 24, LT-03225 Vilnius, Lithuania

ARTICLE INFO

Article history:
Received 31 July 2011
Received in revised form 5 November 2011
Accepted 12 November 2011
Available online 21 November 2011

Keywords:
Ni
Titania
Nanotube
Borohydride
Gold particles

ABSTRACT

Gold aggregates with particle size of a few nanometers have been fabricated on the anodized titania nanotube arrays and flat surfaces by a two-step process which involves nickel electroless deposition followed by spontaneous galvanic displacement of Ni by Au from its chloro-complex solution. The structure, morphology and composition of the fabricated catalysts have been characterized using scanning electron microscopy and energy dispersive X-ray analysis. The catalytic activities of the nanostructured Au(Ni) catalysts preformed on the TiO_2 nanotube arrays and flat surfaces have been investigated towards borohydride oxidation in an alkaline medium by cyclic voltammetry and chrono-techniques. The nanostructured Au(Ni) catalysts on the titania nanotube arrays and flat surfaces exhibit enhanced electrochemical activity and stability towards oxidation of BH_4^- ions in an alkaline medium as compared to that of bulk Au.

1. Introduction

Fuel cells allow direct conversion of chemical energy to electric energy. One type of the fuel cell, a direct borohydride fuel cell (DBFC), has recently been investigated as a potential candidate for portable and mobile applications due to its high energy density and the ease with which borohydride can be stored and transported [1–4]. The DBFC is based on borohydride oxidation:

$$BH_4^- + 8OH^- \rightarrow BO_2^- + 6H_2O + 8e^-, \quad E^\circ = -1.24\,V \tag{1}$$

and oxygen reduction:

$$2O_2 + 4H_2O + 8e^- \rightarrow 8OH^-, \quad E^\circ = 0.40\,V \tag{2}$$

The overall reaction:

$$BH_4^- + 2O_2 \rightarrow BO_2^- + 2H_2O, \quad E^\circ = 1.64\,V \tag{3}$$

Since borohydride is used as fuel, the development of low-cost, stable and highly active electrocatalysts towards borohydride oxidation is of considerable interest. It is well known that gold is an effective electrocatalyst for the oxidation of BH_4^- ions [5–10], however, the use of a noble metal as an electrode material is limited by its high price. One of the ways to reduce amount of Au is to disperse small Au particles (in order of a few nanometers) on a technologically relevant substrate. A variety of nanostructured conducting materials like mesoporous carbon, carbon nanotubes and nanofibers were used as supports for Au catalysts to minimize the use of the precious metal.

This work is focused on the study of self-ordered titania nanotube arrayed (denoted as TiO_2-NTs) and flat (denoted as TiO_2-flat) surfaces as a support for loading of gold particles with the aim to fabricate a highly efficient nano-Au(Ni)/TiO_2-NTs and nano-Au(Ni)/TiO_2-flat electrocatalysts for the oxidation of BH_4^- ions in an alkaline medium. Anodized titania nanotube arrays and flat surfaces as a substrate for the fabrication of catalysts were applied here due to their easy preparation, high orientation, large surface area, high uniformity, non-toxicity, chemical and electrochemical stability and low production costs, which makes them valuable functional materials in many areas [11–17]. Self-ordered titania nanotubed surfaces are an ideal choice of supporting materials for high performance catalysts. Au nanoparticles dispersed over a self-organized nanotubular TiO_2 matrix have been used as a highly efficient catalyst system for the electrochemical oxygen reduction in aqueous solutions [18], electrochemical oxidation of glucose [19,20], water-gas shift reaction [21], degradation of dyes [22,23], CO oxidation [24–27] and others. The Au-modified TiO_2 nanotube arrays also provide excellent matrices for the immobilization of bio molecules in enzyme-attached electrode fabrication [13–15] or for the fabrication of H_2O_2 biosensors [16,17]. Ponce-de-Léon et al. [28] applied the TiO_2 nanotubes as a support for a gold-based electrocatalyst for borohydride oxidation. A variety of methods

* Corresponding author. Tel.: +370 5 2661291; fax: +370 5 2649774.
E-mail address: lortam@ktl.mii.lt (L. Tamašauskaitė-Tamašiūnaitė).

0378-7753/$ – see front matter © 2011 Elsevier B.V. All rights reserved.
doi:10.1016/j.jpowsour.2011.11.030

are used for the metal nanoparticles loading onto the TiO_2-NTs surface. One possibility is that Au/TiO_2-NTs electrodes are prepared by a two-step process of anodization of titanium followed by cathodic electrodeposition of gold on resulted TiO_2 [19,29], by ion-exchange adsorption followed by chemical reduction [28], by an argon plasma technique [16,17]. Another way for fabricating electrodes is focused on the deposition-precipitation methods that were used to load nanoparticles of different metals on the surface of mesoporous titanate nanotubes produced by alkali hydrothermal treatment of TiO_2 [30–33]. These methods are either complex and complicated or high-priced. So, less complicated and simpler methods for the fabrication of catalyst are desirable.

In this work we have successfully fabricated adherent gold-coated nickel films, Au(Ni), with particle size of a few nanometers on anodized titania nanotube arrayed and flat surfaces by a two-step process which involves nickel electroless deposition followed by spontaneous galvanic displacement of Ni by Au from its chloro-complex solution. This simple procedure is based on an electrochemical process, during which the deposition of a noble metal occurs by the oxidation of a precursor metal adlayer deposited on the substrate at the open-circuit potential [34–40]. In this study, the spontaneous oxidation of a Ni adlayer by $AuCl_4^-$ ions has been used to produce Au particles on the self-ordered titania nanotubes arrayed and flat surfaces. The electrocatalytic activity of the prepared catalysts was examined towards borohydride oxidation by cyclic voltammetry (CV), chronoamperometry (CA) and chronopotentiometry (CP). The structure, morphology and composition of the fabricated catalysts were characterized using scanning electron microscopy (SEM) and energy dispersive X-ray (EDAX) analysis.

2. Experimental details

2.1. Chemicals

Titanium foil (99.7% purity of 0.127 mm thickness), $NaBH_4$ and $HAuCl_4$ were purchased from Sigma–Aldrich Supply. H_2SO_4 (96%), NH_4F (97%), NaOH (98.8%), ethanol and acetone were purchased from Chempur Company. All chemicals were of analytical grade. Deionized water was used to prepare all the solutions.

2.2. Fabrication of catalysts

The self-ordered TiO_2 nanotube arrays in this study were prepared by anodic oxidation of Ti foil surface [41]. Briefly, prior to anodization, titanium sheets (1 cm × 1 cm) were degreased with ethanol, rinsed with deionised water and dried in an Ar stream. Titanium sheets were anodized in a 0.24 M H_2SO_4 solution with 0.5 wt.% NH_4F at a constant potential of 20 V at room temperature for 1 h. Two sheets of Pt were used as counter electrodes.

For comparison, flat TiO_2 electrodes were also grown as reference samples by anodizing Ti in (fluoride free) 0.24 M H_2SO_4 at 20 V for 10 min.

To deposit the Au(Ni) catalyst on the TiO_2 nanotube arrayed and flat surfaces, at first, a thin layer of electroless Ni was deposited on them by the following procedures: (a) activation of the TiO_2 nanotube arrayed and flat surfaces in a 0.5 g l^{-1} $PdCl_2$ solution for 60 s; (b) subsequent rinsing of the activated surfaces with deionized water; (c) followed by the immersion of the activated samples into an electroless nickel bath for 60 s. The electroless plating bath consists of 0.1 M nickel sulfate, 0.4 M glycine, 0.25 M sodium hyphophosphite and 0.1 M disodium malonate. The bath operated at pH 9 and a temperature of 85 ± 2 °C. Then the prepared Ni/TiO_2-NTs and Ni/TiO_2-flat electrodes were immersed in a 1 mM $HAuCl_4$ solution (pH 1.8) at room temperature for 60 s. The surface-to-volume ratio was 1.3 dm^2 l^{-1}. After plating, the samples were taken out, thoroughly rinsed with deionized water and air dried at room temperature. Then, the prepared catalysts were used for borohydride electro-oxidation measurements without any further treatment.

2.3. Characterization of catalysts

The surface morphology and composition of the samples were characterized using a Scanning Electron Microscope EVO-50 EP (Carl Zeiss SMT AG, Germany) with Energy Dispersive and Wave dispersion X-ray Spectrometers (Oxford, UK). Metal loading was estimated using STRATAGEM software and EDS K-ratios for Ni, P, Ti and O K alpha lines and Au L alpha lines.

2.4. Electrochemical measurements

A conventional three-electrode electrochemical cell was used for electrochemical measurements. The nano-Au(Ni)/TiO_2-NTs, nano-Au(Ni)/TiO_2-flat, Ni/TiO_2-NTs, TiO_2-NTs catalysts with a geometric area of 2 cm^2 were employed as working electrodes, an Ag/AgCl/KCl electrode was used as a reference electrode and a Pt sheet located in a separate glass-fritted compartment was used as a counter electrode. The electroactive surface area of the counter electrode calculated from the hydrogen adsorption was 7 cm^2. An Au-sputtered quartz crystal with a geometric area of 0.636 cm^2 was used as a bulk gold electrode. Cyclic voltammetry, chronoamperometry and chronopotentiometry experiments were made with a Metrohm Autolab potentiostat (PGSTAT100) using Electrochemical Software (Nova 1.6.013). The presented current densities are normalized with respect to the geometric area of catalysts.

3. Results and discussion

3.1. Physical characterization

Self-ordered TiO_2 nanotube arrays (Fig. 1a) in this study were prepared by anodic oxidation of Ti surface in an aqueous sulfuric acid solution containing NH_4F. The average tube diameter was about 100 nm and the thickness of titania layers was ~350 nm. The electroless Ni–P layer with the thickness of about 300 nm was deposited on the titania nanotube surface, which produces a layer of granular nickel particles about 200 nm in size, as Fig. 1b testifies. It is clearly seen, that immersion of Ni/TiO_2-NTs electrode into the gold-containing solution results in the formation of numerous gold particles on the Ni surface. The Au aggregates appear as bright spots and a statistical analysis of the observed granules indicated they had an average diameter of about 10–30 nm for 1 min Ni/TiO_2-NTs electrode immersion in the gold-containing solution. They are quite uniform in size and well separated. Fig. 1c and d shows SEM micrographs of the TiO_2-flat and nano-Au(Ni)/TiO_2-flat electrodes, respectively. The Au particles in size of 10–30 nm were also detected.

The presence of Au and Ni was confirmed by Energy dispersive X-ray analysis. According to the data of EDAX analysis presented in Table 1 a significant quantity of deposited nickel and a much lower amount of Au on both catalysts surfaces were detected, furthermore, lower amounts of both Ni and Au were deposited on the flat TiO_2 surface.

Also the Au loading in the fabricated catalysts was estimated using STRATAGEM software and EDS K-ratios for Ni, P, Ti and O K alpha lines and Au L alpha lines. It has been determined that after sonication of Ni/TiO_2-flat and Ni/TiO_2-NTs in a gold-containing solution for 1 min, the nano-Au(Ni)/TiO_2-flat and nano-Au(Ni)/TiO_2-NTs catalysts contained the Au loadings of 1.28 and 3.07 μg Au cm^{-2}, respectively.

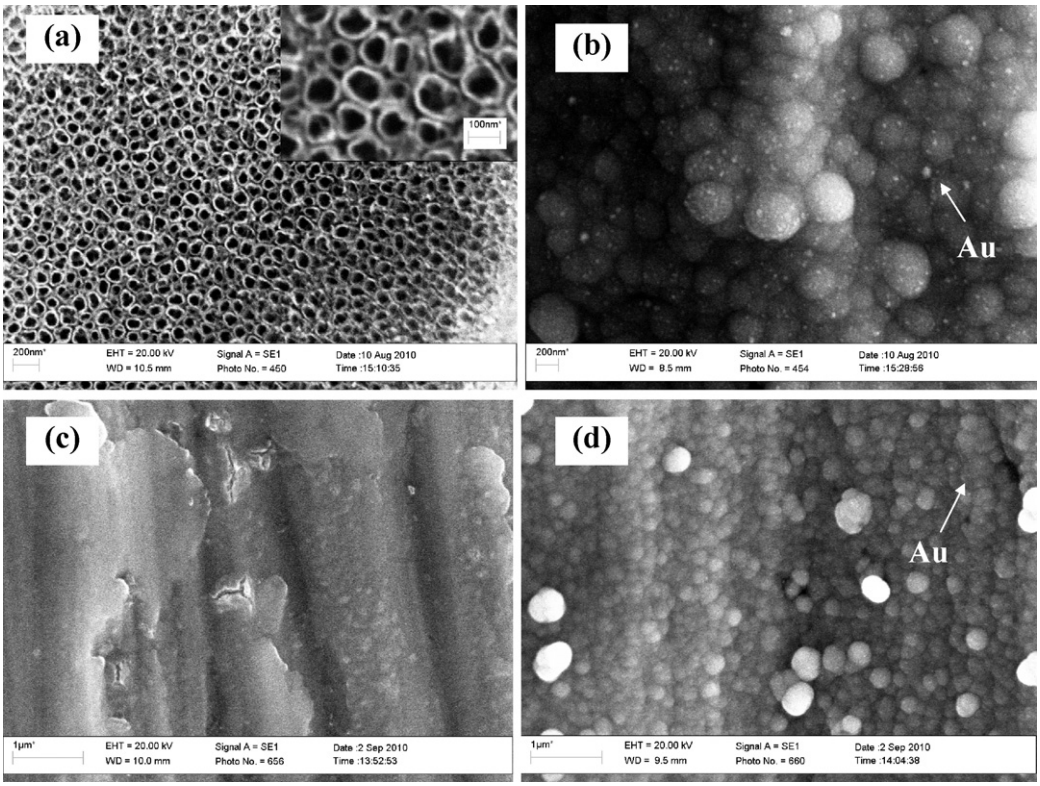

Fig. 1. SEM images of TiO_2-NTs (a), Au(Ni)/TiO_2-NTs (b), TiO_2-flat (c) and Au(Ni)/TiO_2-flat (d).

3.2. Electrochemical catalyst surface characterization

The electroactive area of gold surface created on fabricated catalysts was determined from the cyclic voltammograms of nano-Au/TiO_2-NTs, nano-Au/TiO_2-flat and Au electrodes recorded in a deaerated 0.5 M H_2SO_4 solution at a sweep rate of 100 mV s^{-1} (Fig. 2). The CV profiles of the nano-Au/TiO_2-NTs and nano-Au/TiO_2-flat catalysts show the usual characteristics of Au since Ni–P is electrochemically leached. The gold electroactive surface areas (ESAs) in the catalysts were calculated by the charge associated with the Au surface oxide stripping peak (400 μC cm^{-2}) [42]. The calculated ESAs values for nano-Au/TiO_2-NTs, nano-Au/TiO_2-flat and bare Au are 3.1, 2.3 and 1.6 cm^2, respectively. It should be noticed that the ESAs of catalysts prepared by galvanic displacement of Ni layer by gold particles are ca. two-fold higher than that of bulk Au.

3.3. Cyclic voltammetry oxidation of borohydride

Fig. 3 presents cyclic voltammograms for the oxidation of BH_4^- ions at TiO_2-NTs in 1 M NaOH (*dotted line*) and 0.05 M $NaBH_4$ + 1 M NaOH (*solid line*) solutions at 25 °C with a sweep rate of 10 mV s^{-1}. Fig. 4 shows the CVs for the oxidation of BH_4^- ions at a bare Au (*dotted line*) and Ni/TiO_2-NTs (*dash-dotted line*) in 0.05 M $NaBH_4$ and 1 M NaOH at 25 °C with a sweep rate of 10 mV s^{-1}.The current densities are calculated with respect to the geometric area of catalysts. As evident from Fig. 3 (*dotted line*), the current densities observed on the TiO_2-NTs electrode are negligible in the supporting electrolyte, while in the borohydride solution anodic peaks are seen in the CV with current densities of about 0.01 mA cm^{-2}. In the case of the Ni/TiO_2-NT electrode, during the positive-potential scan in the borohydride solution anodic peak A0 appears at more negative potential values at ca. −0.8 V and it is attributed to H_2 oxidation generated by the catalytic hydrolysis of BH_4^- as described

Table 1
The content of elements onto the surface of the nano-Au(Ni)/TiO_2-NTs (a) and nano-Au(Ni)/TiO_2-flat (b) catalysts obtained by EDAX analysis. The (a) and (b) catalysts were fabricated by the immersion of the TiO_2-NTs and TiO_2-flat surfaces into the nickel bath operated at 85 °C for 60 s followed by their immersion in 1 mM $HAuCl_4$ at pH 1.8 for 60 s.

Catalysts	Elements, at.%				
	Au	Ni	P	O	Ti
(a)	0.76	65.53	9.44	4.77	19.53
(b)	0.52	32.70	3.98	8.65	54.15

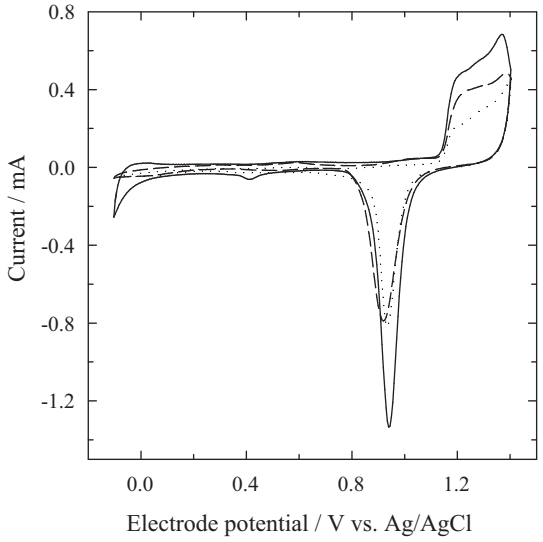

Fig. 2. CVs of bare Au (dotted line), Au(Ni)/TiO_2-NTs (solid line) and Au(Ni)/TiO_2-flat (dashed line) in 0.5 M H_2SO_4 at a sweep rate of 100 mV s^{-1}.

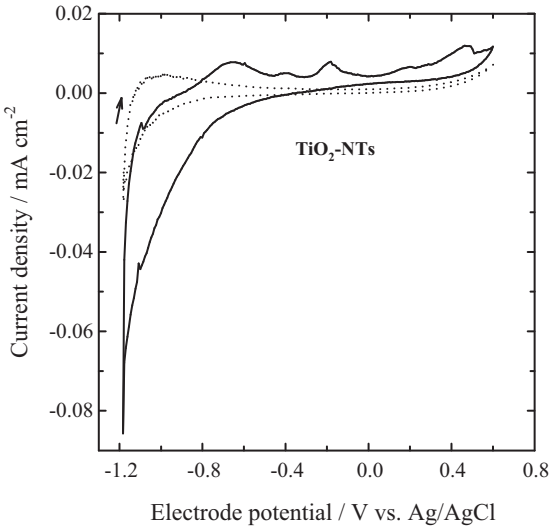

Fig. 3. CVs of TiO_2-NTs in 0.05 M $NaBH_4$ + 1 M NaOH (solid line) and in 1 M NaOH (dotted line) at 25 °C with a sweep rate of 10 mV s^{-1}.

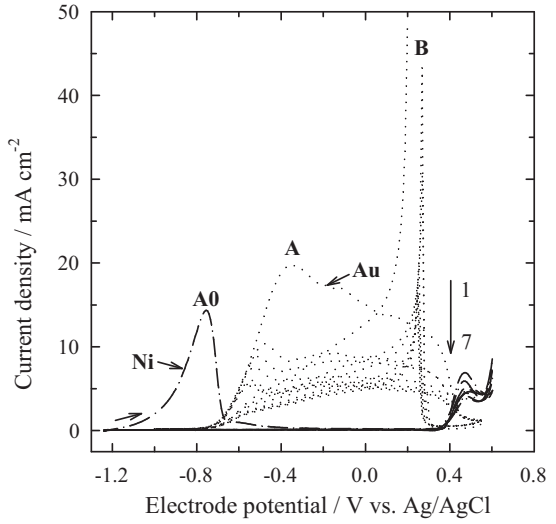

Fig. 4. CVs of bare Au (dotted line) and Ni/TiO_2-NTs (dash-dotted) in 0.05 M $NaBH_4$ + 1 M NaOH at 25 °C with a sweep rate of 10 mV s^{-1}.

in [43–46] (borohydride oxidation releases molecular hydrogen) (Fig. 4, *dash-dotted line*). During the subsequent anodic scans no anodic peaks were observed on this catalyst. It may be proposed that the Ni–P layer deposited on the titania nanotube arrayed surface does not catalyze the direct BH_4^- ions oxidation at higher potentials due to a passivation caused nickel (hydr)oxide(s) formation [47,48] or, maybe, the surface of catalyst is poisoned by strongly adsorbed intermediates generated during the BH_4^- ion oxidation [7].

In the case of bare Au, in the positive potential scan a broad anodic peak A is observed at a potential of −0.4 V (Fig. 4, *dotted line*). This oxidation peak is attributed to the direct oxidation of BH_4^- ions according to Eq. (1) [5–7]. Furthermore, a wide oxidation wave that extends up to 0.4 V corresponds to the oxidation of reaction intermediates on the partially oxidized Au surface [7]. In the reverse scan, a sharp peak B is observed at ca. 0.2 V followed by a plateau in the potential region from 0.0 to −0.6 V. This peak corresponds to the oxidation of adsorbed species such as BH_3OH^- or other borohydrides formed as an intermediate during the oxidation of the BH_4^- ion in the forward scan [6,7].

Fig. 5 shows CV plots vs. the geometric area for the nano-Au(Ni) catalyst deposited on both TiO_2-NTs (a) and TiO_2-flat (b) surfaces. In contrast to borohydride oxidation on the bare Au electrode, in the CVs two well-separated anodic peaks A0 and A are observed (Fig. 5a,b). Since gold is not catalytically active for borohydride hydrolysis [7,43], it may be suggested that electrocatalytic activity of nano-Au(Ni)/TiO_2-NTs and nano-Au(Ni)/TiO_2-flat catalysts at low overpotentials (peak A0) related with H_2 oxidation is due to enhancement of Ni catalytic activity by the presence of Au nanogranules. Since pure TiO_2-NTs and Ni/TiO_2-NTs electrodes do not show electroactivity towards the direct electrooxidation of BH_4^- ions, the observed prominent anodic currents under the potential region of −0.6 and 0.4 V can be ascribed to the electrocatalytic activity of the Au particles deposited on the Ni/TiO_2-NTs and Ni/TiO_2-flat electrodes. Noteworthy that the current densities of peak A for the first anodic scans on the nano-Au(Ni) catalysts deposited on both titania nanotubes and flat surfaces are ca. two-fold higher as compared to that of bulk Au electrode (Fig. 4, *dotted line*). This result may be attributed to a larger specific surface area of the fabricated nano-Au(Ni)/TiO_2-NTs and nano-Au(Ni)/TiO_2-flat electrodes. The potential values of anodic peaks A on both catalysts are shifted to positive potential values for nano-Au(Ni)/TiO_2-NTs catalyst by 0.2 V (Fig. 5a) and for nano-Au(Ni)/TiO_2-flat by 0.5 V (Fig. 5b) as compared to those of bulk Au (Fig. 4, *dotted line*). When comparing the oxidation of BH_4^- ions on the nano-Au(Ni) catalysts deposited on the both titania surfaces (Fig. 5), it is seen that

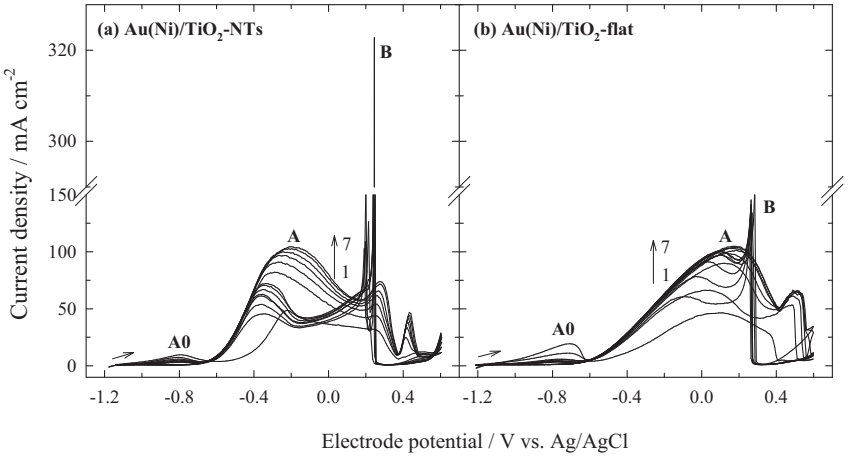

Fig. 5. Long-term CVs of Au(Ni)/TiO_2-NTs (a) and Au(Ni)/TiO_2-flat (b) in 0.05 M $NaBH_4$ + 1 M NaOH at 25 °C with a sweep rate of 10 mV s^{-1}.

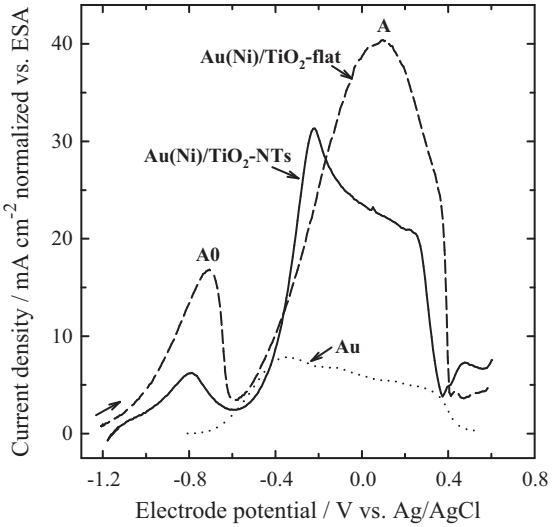

Fig. 6. Positive-potential going CVs of bare Au (dotted line), Au(Ni)/TiO_2-NTs (solid line) and Au(Ni)/TiO_2-flat (dashed line) in 0.05 M $NaBH_4$ + 1 M NaOH at 25 °C with a sweep rate of 10 mV s^{-1}.

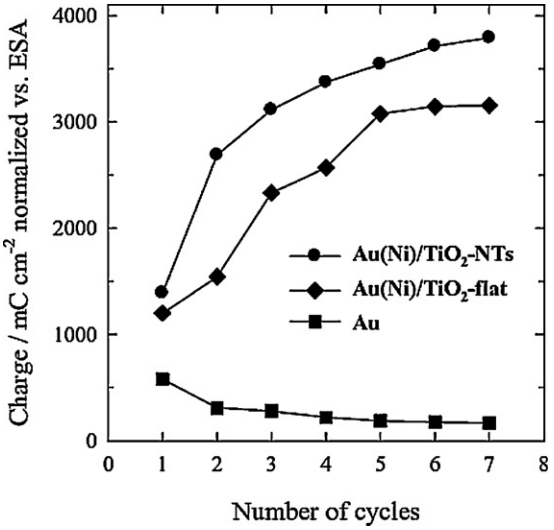

Fig. 7. Charge values calculated from the CVs for bare Au (Fig. 4), Au(Ni)/TiO_2-NTs (Fig. 5a) and Au(Ni)/TiO_2-flat (Fig. 5b) vs. the number of cycles in 0.05 M $NaBH_4$ + 1 M NaOH at 25 °C with a sweep rate of 10 mV s^{-1}.

anodic peak A at nano-Au(Ni)/TiO_2-NTs is observed at more negative potential values than that at nano-Au(Ni)/TiO_2-flat. In the reverse scan, a sharp peak is also observed on these catalysts at about 0.2 V (peak B) much as it is on bare gold.

Fig. 6 presents the comparison of the borohydride oxidation currents after normalization to the active surface area at these catalysts described above. Considering that the active surface areas of nano-Au(Ni)/TiO_2-flat and nano-Au(Ni)/TiO_2-NTs are ca. 1.4–1.9-fold higher compared to Au, the surface area normalized borohydride oxidation current densities are 5.5–4.3 times higher on these catalysts as compared to Au. When comparing the current densities normalized vs. ESA for the Au(Ni) catalysts deposited on both the titania nanotube arrayed and flat surfaces, the active surface area of nano-Au(Ni)/TiO_2-NTs is ca. 1.3-fold higher in comparison to nano-Au(Ni)/TiO_2-flat, the surface area normalized BH_4^- ions oxidation current densities are ca. 1.3 times higher on the nano-Au(Ni)/TiO_2-flat.

The stability of the catalyst performance was also investigated. Long-term potential cycling for Au between −0.8 and 0.6 V (Fig. 4, *dotted line*) and for nano-Au(Ni)/TiO_2-NTs and nano-Au(Ni)/TiO_2-flat between ca. −1.1 and 0.6 V (Fig. 5a,b) was performed for 7 cycles. It is seen that the current densities of BH_4^- ions oxidation (peak A) on the bare gold electrode with respect to the geometric area are decreasing in the subsequent scan cycles. This can probably be due to the formation of intermediates adsorbed on the electrode in the electrocatalytic process, so the poisoned surface of the electrode diminished the electrocatalytic activity of the bare gold electrode [7]. The continuous cyclic voltammetric curves of BH_4^- ion oxidation at the both nano-Au(Ni)/TiO_2-NTs and nano-Au(Ni)/TiO_2-flat catalysts (Fig. 5) show increased catalytic properties in contrast to that of the gold electrode.

The electrical charge for the oxidation of BH_4^- ions at bare Au, nano-Au(Ni)/TiO_2-NTs and nano-Au(Ni)/TiO_2-flat electrodes with respect to the active surface areas under long-term cycling conditions are summarized in Fig. 7. The charge was calculated by integrating the current vs. time under the potential region of about −0.6 and 0.37 V according to the data for bare Au (Fig. 4, *dotted line*) and nano-Au(Ni) catalysts deposited on both the TiO_2-NTs and TiO_2-flat surfaces (Fig. 5). It is clearly seen from Fig. 7, that the corresponded charge for the oxidation of BH_4^- ions after normalization to the active surface area measured on the nano-Au(Ni)/TiO_2-NTs and nano-Au(Ni)/TiO_2-flat catalysts increases with subsequent cycling as compared to that of bulk Au. Additionally, a higher corresponding charge for borohydride oxidation is observed on the nano-Au(Ni) catalyst deposited on the TiO_2 nanotube arrayed surface than the one deposited on the flat TiO_2 surface. Conceivably, the hierarchical structure of TiO_2 nanotube arrays might offer a better accessibility to the active Au particles located at the rim and inside the nanotubes. The BH_4^- ion oxidation peaks are increasing in the subsequent scan cycles, indicating the absence of any significant catalyst losses. According to the obtained results it may be supposed that the nano-Au(Ni)/TiO_2-NTs and nano-Au(Ni)/TiO_2-flat catalysts exhibit a higher electrocatalytic activity for the oxidation of BH_4^- ions and are less sensitive to the poisoning effect of strongly adsorbed species.

3.4. Chronoamperometry and chronopotentiometry in an alkaline borohydride solution

A high electroactivity of nano-Au(Ni) catalysts deposited on both titania surfaces for the oxidation of BH_4^- ions can be further observed from chronoamperometric and chronopotentiometric measurements. Fig. 8 compares chronoamperometry data with respect to the geometric area of catalysts for borohydride oxidation on the nano-Au(Ni)/TiO_2-NTs, nano-Au(Ni)/TiO_2-flat, Ni/TiO_2-NTs, Ni/TiO_2-flat and Au catalysts in 0.05 M $NaBH_4$ and 1 M NaOH at 25 °C. Following a rest period of 10 s at open circuit, the electrode potential was stepped to −0.3 V for 120 s. The nano-Au(Ni)/TiO_2-NTs, nano-Au(Ni)/TiO_2-flat and Au catalysts show a current decay for the oxidation of BH_4^- ions. At the end of experimental period (t = 130 s), the current densities of the nano-Au(Ni) catalyst deposited on the titania nanotube arrayed surface are about two-fold higher than that on the flat titania surface and ca. 20-fold higher than that at bare Au. Also ca. ten-fold higher current densities are observed at the nano-Au(Ni)/TiO_2-flat catalyst as compared to that at Au. Assuming ca. two-fold higher active surface areas of nano-Au(Ni)/TiO_2-NTs and nano-Au(Ni)/TiO_2-flat compared to bulk Au, the surface area normalized BH_4^- ion oxidation currents are ca. 10.9 and 7.6 times higher on those catalysts. The nano-Au(Ni)/TiO_2-NTs and nano-Au(Ni)/TiO_2-flat catalysts have a higher catalytic activity and a better stability for the oxidation of borohydride than bare Au. This result is in agreement with the results of cyclic voltammetry curves.

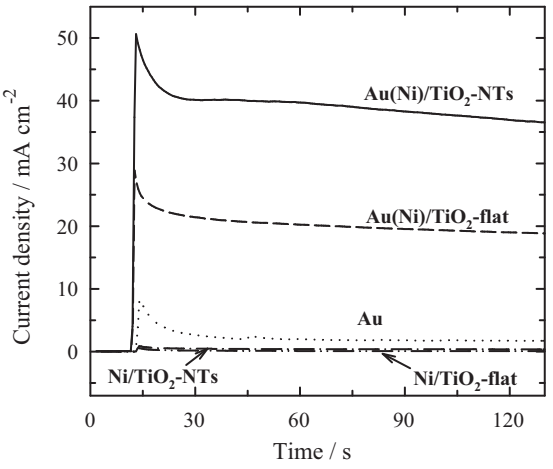

Fig. 8. Chronoamperometry curves of the Au(Ni)/TiO_2-NTs (solid line), Au(Ni)/TiO_2-flat (dashed line), Ni/TiO_2-NTs (dash-dotted), Ni/TiO_2-flat (dash-dot-dotted line) and Au (dotted line) catalysts in 0.05 M $NaBH_4$ + 1 M NaOH at 25 °C. The potential was held at open circuit for 10 s, then set to −0.3 V for 2 min.

The current densities of about 0.2-0.4 mA cm^{-2} obtained on both the Ni/TiO_2-flat and Ni/TiO_2-NTs catalysts under investigated chronoamperometric conditions suggest that latter catalysts are not active for the oxidation of borohydride.

Chronopotentiometric measurements of oxidation of BH_4^- ions were also carried out on the nano-Au(Ni)/TiO_2-NTs, nano-Au(Ni)/TiO_2-flat, Ni/TiO_2-NTs, Ni/TiO_2-flat and Au catalysts. Following a rest period of 10 s at open circuit, a current density step of 10 mA cm^{-2} vs. the geometric area of catalysts was applied to the investigated catalysts for 120 s exposed to a 0.05 M $NaBH_4$ solution in 1 M NaOH at 25 °C. Fig. 9 shows anode potentials (including open-circuit values between −1.16 and −0.54 V) for the catalysts operating at current density of 10 mA cm^{-2}. Notably, the open-circuit potential of composite Au–Ni catalysts are mainly determined by Ni-catalyzed borohydride oxidation in reaction with water to borate as found from the most negative OCP values for Au-free catalysts. The presence of Au particles on the Ni film only slightly shifts the OCP to more positive values, which are, however, still ca. 0.6 V more negative compared to Au electrode. After 120 s the operating potentials for nano-Au(Ni)/TiO_2-flat and nano-Au(Ni)/TiO_2-NTs are up to about 0.262 and 0.268 V more negative

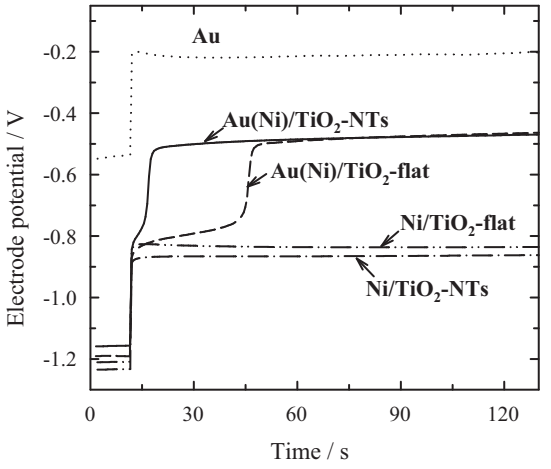

Fig. 9. Chronopotentiometry curves of the Au(Ni)/TiO_2-NTs (solid line), Au(Ni)/TiO_2-flat (dashed line), Ni/TiO_2-NTs (dash-dotted), Ni/TiO_2-flat (dash-dot-dotted line) and Au (dotted line) catalysts in 0.05 M $NaBH_4$ + 1 M NaOH at 25 °C. The current step was from 0 to 10 mA cm^{-2}.

as compared to Au, which demonstrates that the overpotentials for the oxidation of BH_4^- ions on the latter catalysts are lower than that of Au. It is worth mentioning that the operation potentials attained during borohydride oxidation at a current density of 10 mA cm^{-2} over composite Au–Ni catalysts exhibit nearly complete additivity of the values reached on Au-free Ni and that for Au electrode. Furthermore, the operation potential of the composite catalysts is comparable to the OCP value of the Au electrode, whereas the operation potential of the latter is nearly 0.3 V more positive, compared to Au–Ni catalysts. Therefore, the nano-Au(Ni)/TiO_2-NTs and nano-Au(Ni)/TiO_2-flat catalysts may have higher direct electrooxidation activities and power output than those on Au catalyst. The nanostructured Au catalyst may exhibit a higher activity, compared to the extended Au electrode, due to a great number of defect sites and undercoordinated surface atoms as well as the Au–Ni support interactions.

More negative overpotentials values of about 0.634 and 0.659 V are observed on the Ni/TiO_2-flat and Ni/TiO_2-NTs catalysts, respectively, as compared to gold. Assuming that these two catalysts do not show activity towards direct oxidation of BH_4^- ions, it may be suggested that the catalysts operated at 10 mA cm^{-2} initiate only hydrolysis of BH_4^- ions, which occurs with evolution of H_2 followed by its oxidation at a lower potentials of −0.8 V.

The voltammetric performance, chronoamperometry and chronopotentiometry studies confirm that the deposited Au(Ni) catalysts with particle size of a few nanometers on the self-ordered titania nanotube arrayed and flat surfaces exhibit a high electrocatalytic activity towards oxidation of BH_4^- ions. The TiO_2 nanotube arrayed and flat surfaces apparently allow us to form the nanostructured Au(Ni)/TiO_2-NTs and Au(Ni)/TiO_2-flat catalysts with a significantly larger surface area, and, hence, achieve higher oxidation rates in borohydride fuel cells as compared to the bulk Au electrode. The self-ordered titania nanotube arrays and flat surfaces are a promising support for fuel cell catalysts.

4. Conclusions

Gold aggregates with particle size of a few nanometers have been deposited on the anodized titania nanotube arrays and flat surfaces by a two-step process which involves nickel electroless deposition followed by spontaneous galvanic displacement of Ni by Au from its chloro-complex solution. The structure, morphology, composition and electrocatalytic performance of the fabricated catalysts were investigated by scanning electron microscopy, cyclic voltammetry, chronoamperometry and chronopotentiometry.

It has been determined that the nano-Au(Ni)/TiO_2-flat and nano-Au(Ni)/TiO_2-NTs catalysts with the Au loadings of 1.28 and 3.07 μg Au cm^{-2}, respectively, exhibit an enhanced electrochemical activity and stability towards oxidation of BH_4^- ions in an alkaline medium as compared to that of bulk Au. The electrocatalytic properties of the investigated nano-Au(Ni)/TiO_2-NTs and nano-Au(Ni)/TiO_2-flat catalysts increased with the number of scan cycles.

The chronoamperometry and chronopotentiometry studies also confirmed a higher catalytic activity of the nano-Au(Ni)/TiO_2-NTs and nano-Au(Ni)/TiO_2-flat catalysts for the oxidation of BH_4^- ions as compared with that of bulk Au.

The self-ordered titania nanotube arrays and flat surfaces seem to be a promising support for fuel cell catalysts.

Acknowledgements

This research was funded by a grant (No. ATE-03/2010) from the Research Council of Lithuania. A. Balčiūnaitė also acknowledges Student Research Fellowship Award from the Research Council of

Lithuania. We gratefully thank Habil. Dr. Zenonas Jusys from the Institute of Surface Chemistry and Catalysis, Ulm University for helpful discussions.

References

[1] C. Celik, S.F.G. Boyaci, H.I. Sarac, J. Power Sources 185 (2008) 197–201.
[2] C. Celik, S.F.G. Boyaci, H.I. Sarac, J. Power Sources 195 (2010) 599–603.
[3] C.P. de Leon, F.C. Walsh, D. Pletcher, D.J. Browning, J.B. Lakeman, J. Power Sources 155 (2006) 172–181.
[4] S.C. Amendola, P. Onnerud, M.T. Kelly, P.J. Petillo, S.L. Sharp-Goldman, M. Binder, J. Power Sources 84 (1999) 130–133.
[5] M.V. Mirkin, A.J. Bard, Anal. Chem. 63 (1991) 532–533.
[6] M.V. Mirkin, H. Yang, A.J. Bard, J. Electrochem. Soc. 139 (1992) 2212–2217.
[7] E. Gyenge, Electrochim. Acta 49 (2004) 965–978.
[8] H. Cheng, K. Scott, Electrochim. Acta 51 (2006) 3429–3433.
[9] M. Chatenet, F. Micoud, I. Roche, E. Chainet, Electrochim. Acta 51 (2006) 5459–5467.
[10] M.H. Atwan, C.L.B. Macdonald, D.O. Northwood, E.L. Gyenge, J. Power Sources 158 (2006) 36–44.
[11] K. Shankar, G.K. Mor, H.E. Prakasam, S. Yoriya, M. Paulose, O.K. Varghese, C.A. Grimes, Nanotechnology 18 (2007) 1–11.
[12] L.X. Yang, D.M. He, Q.Y. Cai, J. Phys. Chem. C 111 (2007) 8214–8217.
[13] H.E. Prakasam, K. Shankar, M. Paulose, O.K. Varghese, C.A. Grimes, J. Phys. Chem. C 111 (2007) 7235–7241.
[14] Y. Xie, L. Zhou, H. Huang, Biosens. Bioelectron. 22 (2007) 2812–2818.
[15] F. Wu, J. Xu, Y. Tian, Zh. Hu, L. Wang, Y. Xian, L. Jin, Biosens. Bioelectron. 24 (2008) 198–203.
[16] A.K.M. Kafi, G. Wu, A. Chen, Biosens. Bioelectron. 24 (2008) 566–571.
[17] Y. Wang, X. Ma, Y. Wen, Y. Xing, Z. Zhang, H. Yang, Biosens. Bioelectron. 25 (2010) 2442–2446.
[18] J.M. Macak, F. Schmidt-Stein, P. Schmuki, Electrochem. Commun. 9 (2007) 1783–1787.
[19] M. Hosseini, M.M. Momeni, J. Solid State Electrochem. 14 (2010) 1109–1115.
[20] P. Benvenuto, A.K.M. Kafi, A. Chen, J. Electroanal. Chem. 627 (2009) 76–81.
[21] V. Idakiev, Z.Y. Yuan, T. Tabakova, B.L. Su, Appl. Catal. A 281 (2005) 149–155.
[22] Q. Zhao, M. Li, J. Chu, T. Jiang, H. Yin, Appl. Surf. Sci. 255 (2009) 3773–3778.
[23] I. Paramasivam, J.M. Macak, P. Schmuki, Electrochem. Commun. 10 (2008) 71–75.
[24] B. Zhu, Q. Guo, X. Huang, Sh. Wang, Sh. Zhang, Sh. Wu, W. Huang, J. Mol. Catal. A: Chem. 249 (2006) 211–217.
[25] X. Liu, T.F. Jaramillo, J. Mater. Res. 20 (2005) 1093–1096.
[26] J. Jiang, Q. Gao, Zh. Chen, J. Mol. Catal. A: Chem. 280 (2008) 233–239.
[27] T.A. Ntho, J.A. Anderson, M.S. Scurrell, J. Catal. 261 (2009) 94–100.
[28] C. Ponce-de-Léon, D.V. Bavykin, F.C. Walsh, Electrochem. Commun. 8 (2006) 1655–1660.
[29] M. Hosseini, M.M. Momeni, M. Faraji, J. Appl. Electrochem. 40 (2010) 1421–1427.
[30] D.V. Bavykin, A.A. Lapkin, P.K. Plucinski, L. Torrente-Murciano, J.M. Friedrich, F.C. Walsh, Top. Catal. 39 (2006) 151–160.
[31] J.Zh. Xu, W.B. Zhao, J.J. Zhu, G.X. Li, H.Y. Chen, J. Colloid Interface Sci. 290 (2005) 450–454.
[32] B.L. Zhu, Z.M. Sui, X. Chen, S.R. Wang, S.M. Zhang, S.H. Wu, W.P. Huang, Chin. Sci. Bull. 50 (2005) 711–713.
[33] B. Zhu, Zh. Sui, Sh. Wang, X. Chen, Sh. Zhang, Sh. Wu, W. Huang, Mater. Res. Bull. 41 (2006) 1097–1104.
[34] S.R. Brankovic, J. McBreen, R.R. Adzic, J. Electroanal. Chem. 503 (2001) 99–104.
[35] K. Sasakia, J.X. Wang, H. Naohara, N. Marinkovic, K. More, H. Inada, R.R. Adzic, Electrochim. Acta 55 (2010) 2645–2652.
[36] D. Gokcen, S.E. Bae, S.R. Brankovic, J. Electrochem. Soc. 157 (2010) D582–D587.
[37] D. Gokcen, S.E. Bae, S.R. Brankovic, Electrochim. Acta 56 (2011) 5545–5553.
[38] S. Papadimitriou, A. Tegou, E. Pavlidou, S. Armyanov, E. Valova, G. Kokkinidis, S. Sotiropoulos, Electrochim. Acta 53 (2008) 6559–6567.
[39] A. Tegou, S. Armyanov, E. Valova, O. Steenhaut, A. Hubin, G. Kokkinidis, S. Sotiropoulos, J. Electroanal. Chem. 634 (2009) 104–110.
[40] A. Tegou, S. Papadimitriou, I. Mintsouli, S. Armyanov, E. Valova, G. Kokkinidis, S. Sotiropoulos, Catal. Today 170 (2011) 126–133.
[41] T. Tian, X. Xiao, R. Liu, H. She, X. Hu, J. Mater. Sci. 42 (2007) 5539–5543.
[42] H. Angerstein-Kozlowska, B.E. Conway, A. Hamelin, L. Stoicoviciu, Electrochim. Acta 31 (1986) 1051–1061.
[43] B.H. Liu, Z.P. Li, S. Suda, J. Electrochem. Soc. 150 (2003) A398–A402.
[44] B.H. Liu, Z.P. Li, S. Suda, Electrochim. Acta 49 (2004) 3097–3105.
[45] K.M. Gorbunova, M.V. Ivanov, V.P. Moiseev, J. Electrochem. Soc. 120 (1973) 613–618.
[46] J.S. Walter, A. Zurawski, D. Montgomery, M. Thornburg, S. Revankar, J. Power Sources 179 (2008) 335–339.
[47] Ch. Zhang, S.M. Park, J. Electrochem. Soc. 134 (1987) 2966–2970.
[48] M. Wehrens-Dijksma, P.H.L. Notten, Electrochim. Acta 51 (2006) 3609–3621.